Investigating the Theory, Optics and detector for WISP detection in ALPS

Yixuan Zhang

Imperial College London

DESY

Supervisor: Dr. Axel Lindner

Contents

- 1. Introduction
- 2. Theory
  - 2.1 Light shining through a wall with B=0
  - 2.2 ALPS sensitivity for detecting WISPs
- 3. Optics
  - 3.1 Research on production cavity
  - 3.2 Coupling photons into an optical fibre
  - 3.3 A game designed and built for DESY open day
- 4. Detector
  - 4.1 Investigation of the black body photons sources
  - 4.2 Other tests for the detector
- 5. Summary

1. Introduction

- Many evidence from astronomy observation predicts that 25% of the universe is made up of dark matter (DM).
- The weakly interacting slim particle (WISP) is one of the candidates of DM.
- WISPs might arise as (pseudo) Goldstone bosons related to extra dimensions in theoretical extensions (like string theory) of the standard model.

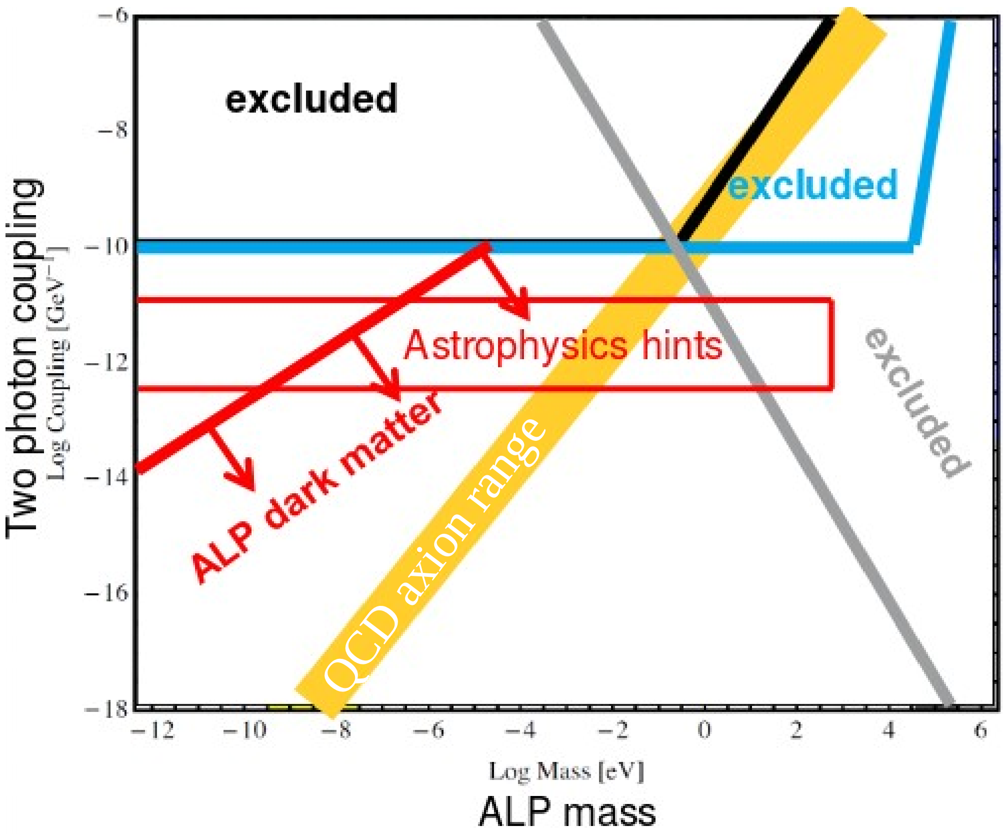

Figure 1: Big picture for searching WISPs.

- WISP particles predicted by theory:
  - ➢ Axions and axion-like particles(ALPs), pseudoscalar or scalar bosons
  - ➢ Hidden photons, neutral vector bosons
  - ➢ Mini-charged particles
  - ➢ Chamleons, massive gravity scalars

2. Theory

- A "hidden sector" of particles is predicted by many theories from the extension of Standard Model and they interact very weakly with the "visible sector" of particles i.e. the SM particles.
- The WISPs arise from spontaneous breakdown of global symmetries.
- We start with a Lagrangian allowed by symmetry

$$L = -\frac{1}{4} F^{\mu\nu} F_{\mu\nu} - \frac{1}{4} B^{\mu\nu} B_{\mu\nu} - \frac{1}{2} \chi F^{\mu\nu} B_{\mu\nu}$$

  where $F_{\mu\nu}$ is the field strength tensor for the visible sector , ($B_{\mu\nu}$) is the field strength tensor for the hidden sector χ is an arbitrary parameter at low energy scale.

- Then we introduce a mass term to break the symmetry:

$$L_{\mu} = \frac{1}{2} \mu^2 B^{\mu} B_{\mu}$$

  where μ is the mass of the hidden photons via Higgs mechanism.

- We can generalise the Lagrangian, and by diagonalising the whole expression we can obtain the mass mixing term

$$L = -\frac{1}{4} F^T \mathrm{K} F + \frac{1}{2} A^T \mathrm{M} A \quad \text{with} \quad \mathrm{K} = \begin{pmatrix} 1 & \chi & \chi \\ \chi & 0 & 0 \\ \chi & 0 & 0 \end{pmatrix} \quad \mathrm{M} = \begin{pmatrix} 0 & 0 & 0 \\ 0 & \mu^2 & 0 \\ 0 & 0 & 0 \end{pmatrix} \quad => \quad \widetilde{\mathrm{M}} = \begin{pmatrix} \chi^2 \mu^2 & -\chi \mu^2 & 0 \\ -\chi \mu^2 & \mu^2 & 0 \\ 0 & 0 & 0 \end{pmatrix}$$

2. Theory

- A “hidden sector” of particles is predicted by many theories from the extension of Standard Model and they interact very weakly with the “visible sector” of particles i.e. the SM particles.

- The WISPs arise from spontaneous breakdown of global symmetries.

- We start with a Lagrangian allowed by symmetry

$$L = -\frac{1}{4} F^{\mu\nu} F_{\mu\nu} - \frac{1}{4} B^{\mu\nu} B_{\mu\nu} - \frac{1}{2} \chi F^{\mu\nu} B_{\mu\nu}$$

  where $F_{\mu\nu}$ is the field strength tensor for the visible sector , ($B_{\mu\nu}$) is the field strength tensor for the hidden sector χ is an arbitrary parameter at low energy scale.

- Then we introduce a mass term to break the symmetry:

$$L_{\mu} = \frac{1}{2} \mu^2 B^{\mu} B_{\mu}$$

  where μ is the mass of the hidden photons via Higgs mechanism.

- We can generalise the Lagrangian, and by diagonalising the whole expression we can obtain the mass mixing term

$$L = -\frac{1}{4} F^T \mathrm{K} F + \frac{1}{2} A^T \mathrm{M} A \quad \text{with} \quad \mathrm{K} = \begin{pmatrix} 1 & \chi & \chi \\ \chi & 0 & 0 \\ \chi & 0 & 0 \end{pmatrix} \quad \mathrm{M} = \begin{pmatrix} 0 & 0 & 0 \\ 0 & \mu^2 & 0 \\ 0 & 0 & 0 \end{pmatrix} \quad \Rightarrow \quad \tilde{\mathrm{M}} = \begin{pmatrix} \chi^2 \mu^2 & -\chi \mu^2 & 0 \\ -\chi \mu^2 & \mu^2 & 0 \\ 0 & 0 & 0 \end{pmatrix}$$

2.1 Light shining through a wall with B=0

- By writing down the equation of motion, we are able to obtain the probability of a photon propagating via this diagram:

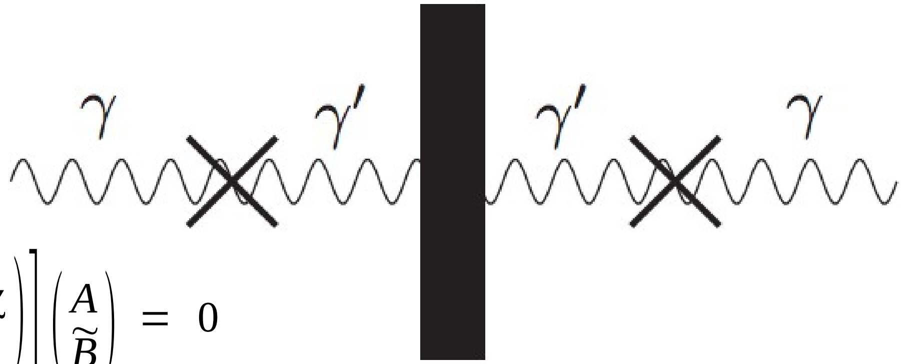

Figure 2: LSW with photon converting to hidden photon and recombined behind the wall

$$[(\omega+\partial_z^2)\mathrm{I}-\mu^2\tilde{\mathrm{M}}]\begin{pmatrix}A\\ \tilde{B}\end{pmatrix} = \left[(\omega+\partial_z^2)\begin{pmatrix}1 & 0\\ 0 & 1\end{pmatrix}-\mu^2\begin{pmatrix}\chi^2 & -\chi\\ -\chi & 1\end{pmatrix}\right]\begin{pmatrix}A\\ \tilde{B}\end{pmatrix} = 0$$

- The eigenstates can be found to be

$$\nu_1 = \begin{pmatrix}1\\ \chi\end{pmatrix}\exp(-i(\omega t \pm k_1 z)) \quad \text{with} \quad k_1^2=\omega^2$$

$$\nu_2 = \begin{pmatrix}-\chi\\ 1\end{pmatrix}\exp(-i(\omega t \pm k_2 z)) \quad \text{with} \quad k_2^2=\omega^2-\mu^2-\cancel{\mu^2\chi^2}$$

- So a superposition of these eigenstates in the initial state can be formed

$$V(0,0)=A_0\begin{pmatrix}1\\ 0\end{pmatrix}=A_0\left(\frac{1}{1+\chi^2}\nu_1(0,0)-\frac{\chi}{1+\chi^2}\nu_2(0,0)\right)$$

And the probability of a photon converting into a hidden photon will be

$$P_{\gamma\to\gamma'}(z)=1-P_{\gamma\to\gamma}(z)=4\chi^2\sin^2\left(\frac{\mu^2}{2\omega}z\right)=P_{\gamma'\to\gamma}(z)$$

- Thus, the probability of one reconverted photon detection will be

$$P_{trans}=P_{\gamma\to\gamma'}P_{\gamma'\to\gamma}=16\chi^4\sin^2\left(\frac{\mu^2 l_1}{2}\right)\sin^2\left(\frac{\mu^2 l_2}{2}\right)$$

2.2 ALPS sensitivity for detecting WISPs

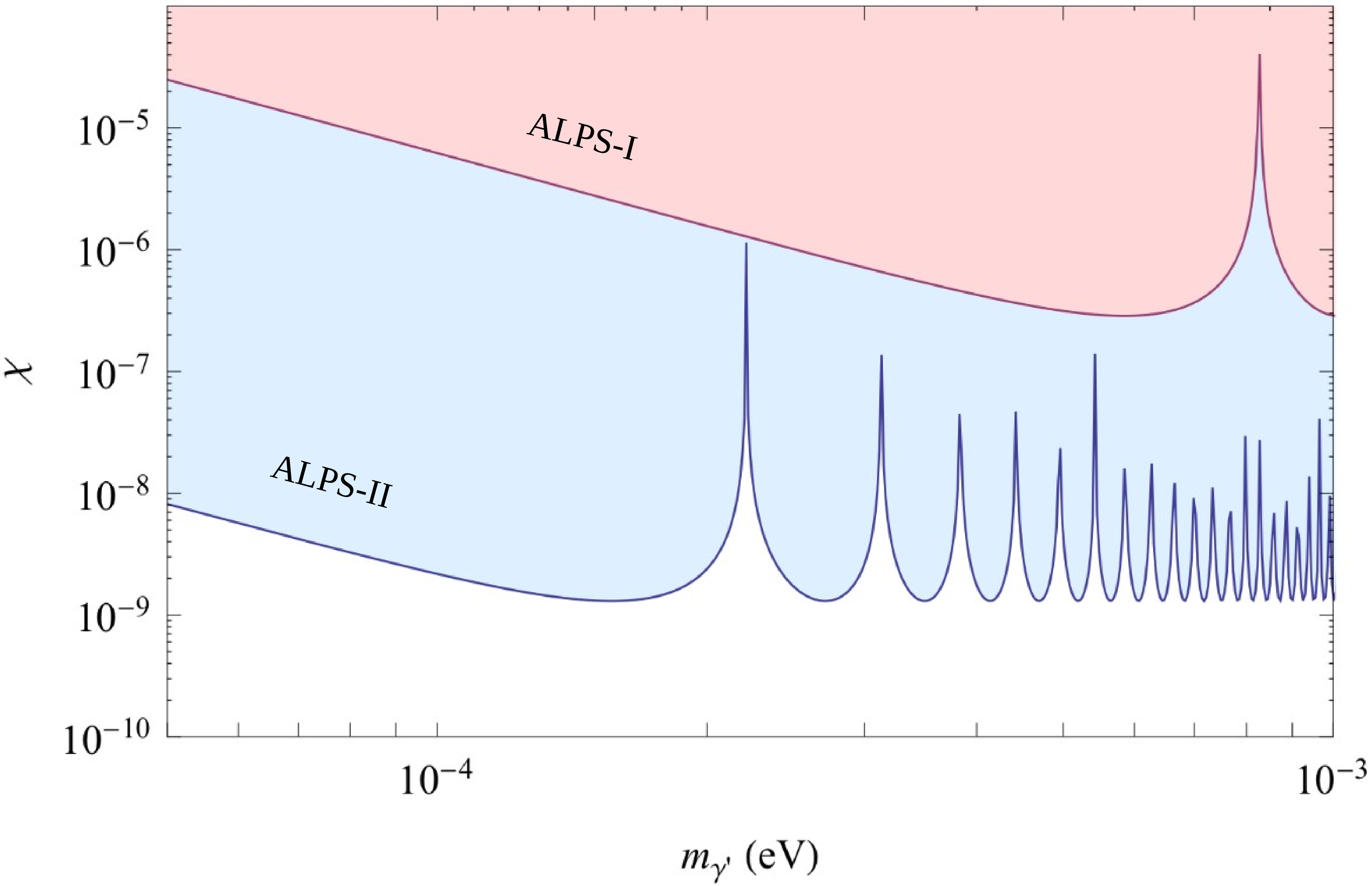

Figure 3: Hidden photon searches with LSW experiment for ALPS. The red region is the best sensitivity for ALPS-I and the blue region is for ALPS-II.

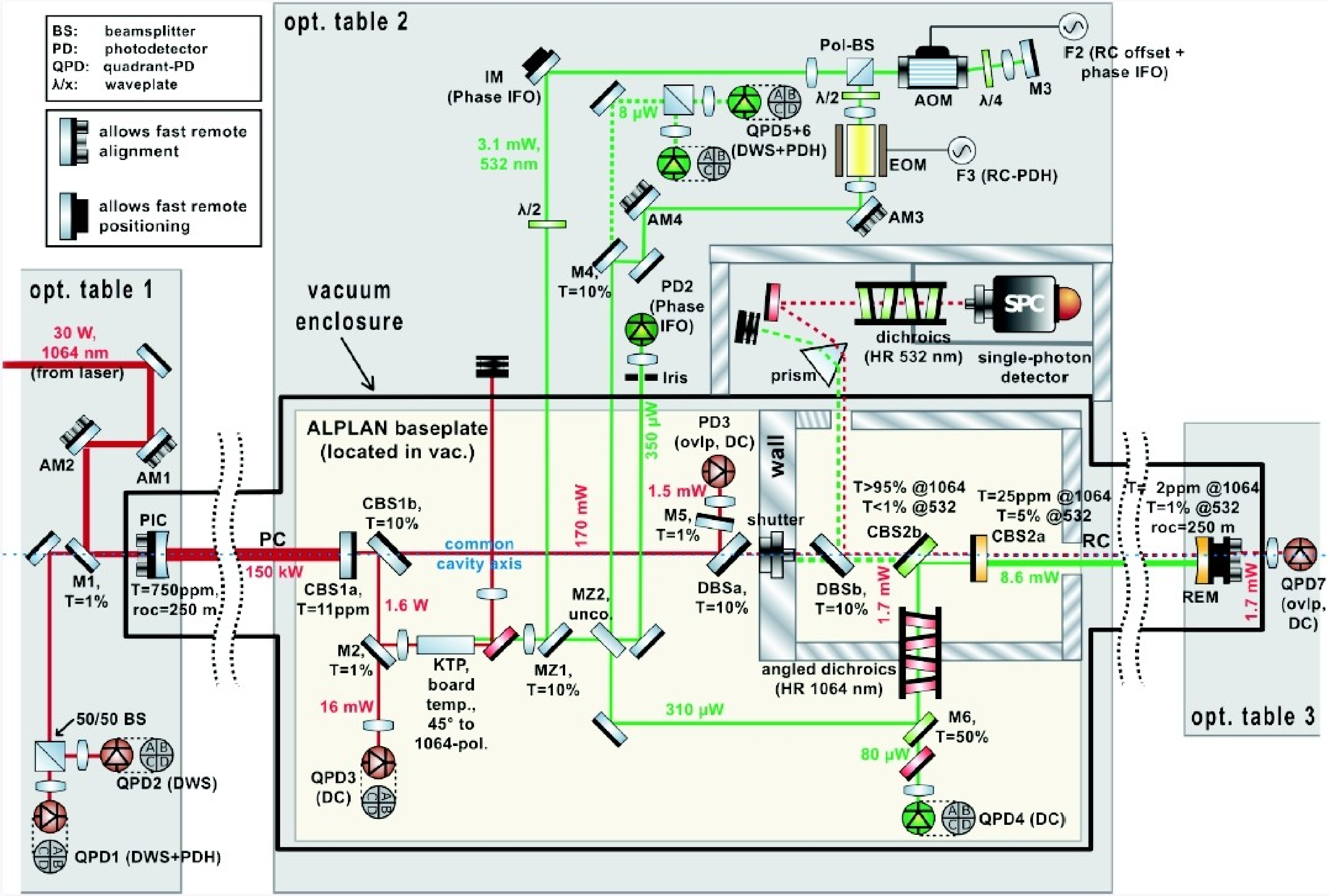
BS: beamsplitter
PD: photodetector
QPD: quadrant-PD
λ/x: waveplate
allows fast remote alignment
allows fast remote positioning
opt. table 1
30 W, 1064 nm (from laser)
AM2
AM1
M1, T=1%
PIC
T=750ppm, roc=250 m
50/50 BS
QPD2 (DWS)
QPD1 (DWS+PDH)
opt. table 2
vacuum enclosure
IM (Phase IFO)
3.1 mW, 532 nm
λ/2
8 µW
QPD5+6 (DWS+PDH)
Pol-BS
λ/2
AOM
λ/4
M3
F2 (RC offset + phase IFO)
EOM
F3 (RC-PDH)
AM4
AM3
M4, T=10%
PD2 (Phase IFO)
Iris
dichroics (HR 532 nm)
SPC
single-photon detector
prism
ALPLAN baseplate (located in vac.)
PC
150 kW
CBS1b, T=10%
CBS1a, T=11ppm
common cavity axis
170 mW
350 µW
1.6 W
M2, T=1%
16 mW
QPD3 (DC)
KTP, board temp., 45° to 1064-pol.
MZ1, T=10%
MZ2, unco.
PD3 (ovlp, DC)
1.5 mW
M5, T=1%
DBSa, T=10%
wall
shutter
DBSb, T=10%
1.7 mW
T>95% @1064
T<1% @532
CBS2b
T=25ppm @1064
T=5% @532
CBS2a
RC
8.6 mW
angled dichroics (HR 1064 nm)
310 µW
M6, T=50%
80 µW
QPD4 (DC)
T= 2ppm @1064
T=1% @532
roc=250 m
REM
1.7 mW
QPD7 (ovlp, DC)
opt. table 3

3. Optics

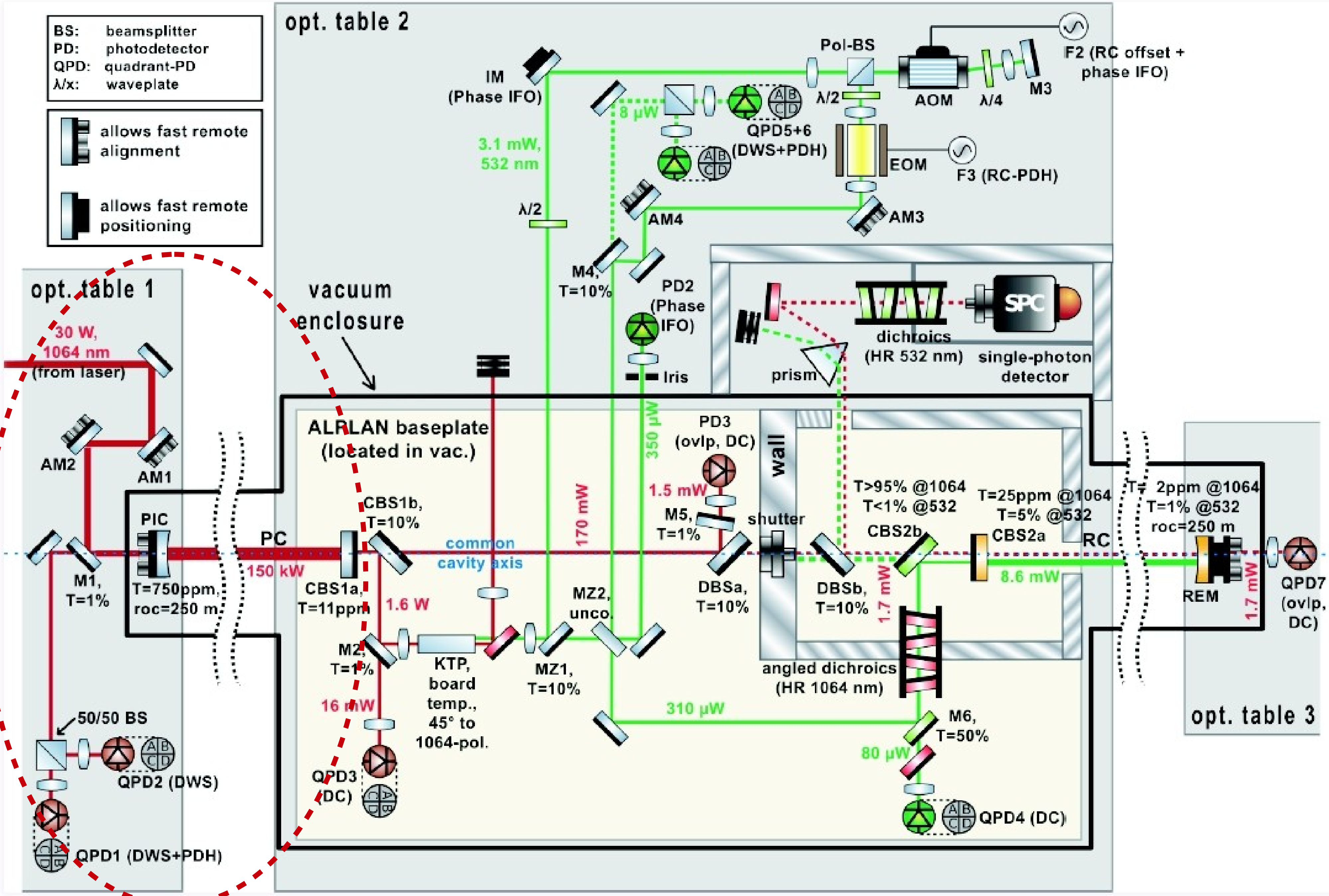

BS: beamsplitter
PD: photodetector
QPD: quadrant-PD
λ/x: waveplate
allows fast remote alignment
allows fast remote positioning
opt. table 1
opt. table 2
opt. table 3
30 W, 1064 nm (from laser)
AM1
AM2
M1, T=1%
PIC
T=750ppm, roc=250 m
PC
150 kW
50/50 BS
QPD2 (DWS)
QPD1 (DWS+PDH)
vacuum enclosure
ALPLAN baseplate (located in vac.)
CBS1b, T=10%
CBS1a, T=11ppm
common cavity axis
1.6 W
M2, T=1%
16 mW
QPD3 (DC)
KTP, board temp., 45° to 1064-pol.
MZ1, T=10%
MZ2, unco.
170 mW
350 μW
310 μW
IM (Phase IFO)
3.1 mW, 532 nm
λ/2
8 μW
QPD5+6 (DWS+PDH)
Pol-BS
λ/2
AOM
λ/4
M3
F2 (RC offset + phase IFO)
EOM
F3 (RC-PDH)
AM3
AM4
M4, T=10%
PD2 (Phase IFO)
Iris
prism
dichroics (HR 532 nm)
SPC
single-photon detector
PD3 (ovlp, DC)
1.5 mW
M5, T=1%
DBSa, T=10%
wall
shutter
DBSb, T=10%
T>95% @1064
T<1% @532
CBS2b
1.7 mW
T=25ppm @1064
T=5% @532
CBS2a
8.6 mW
T= 2ppm @1064
T=1% @532
roc=250 m
RC
REM
1.7 mW
QPD7 (ovlp, DC)
angled dichroics (HR 1064 nm)
M6, T=50%
80 μW
QPD4 (DC)

3.1 Research on production cavity - Problem

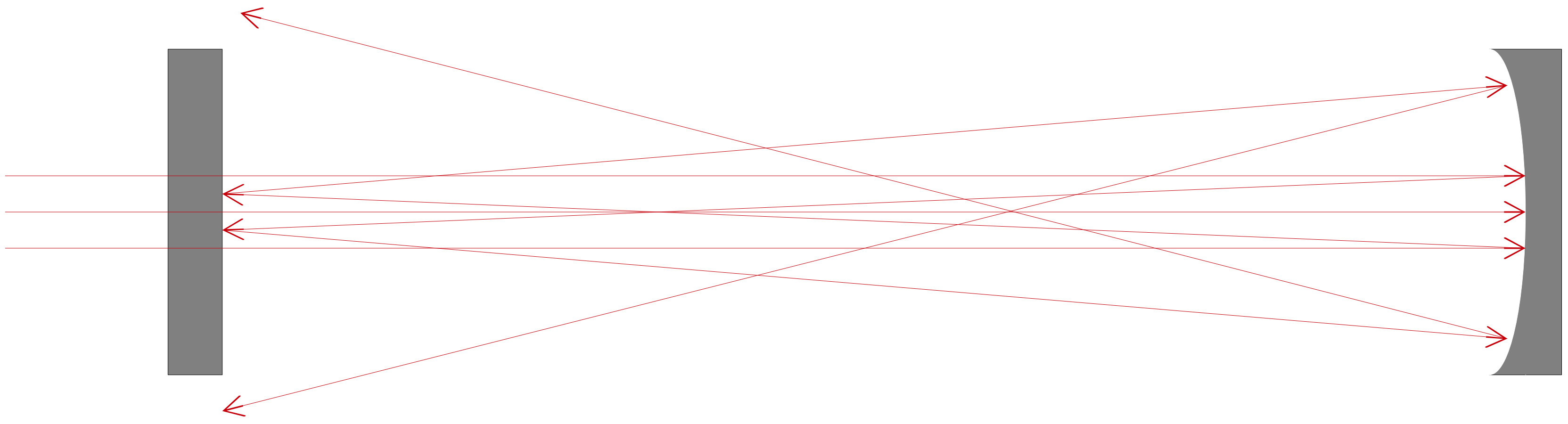

Figure 4: Potential problem of the missing laser intensity

- The production cavity was 10m long with photon wavelength of 1064nm.
- Problem with missing intensity inside the cavity.
- Hypothesis of causes has been raised and need to be tested.
- Therefore, a model with 10cm long cavity was built for investigation.

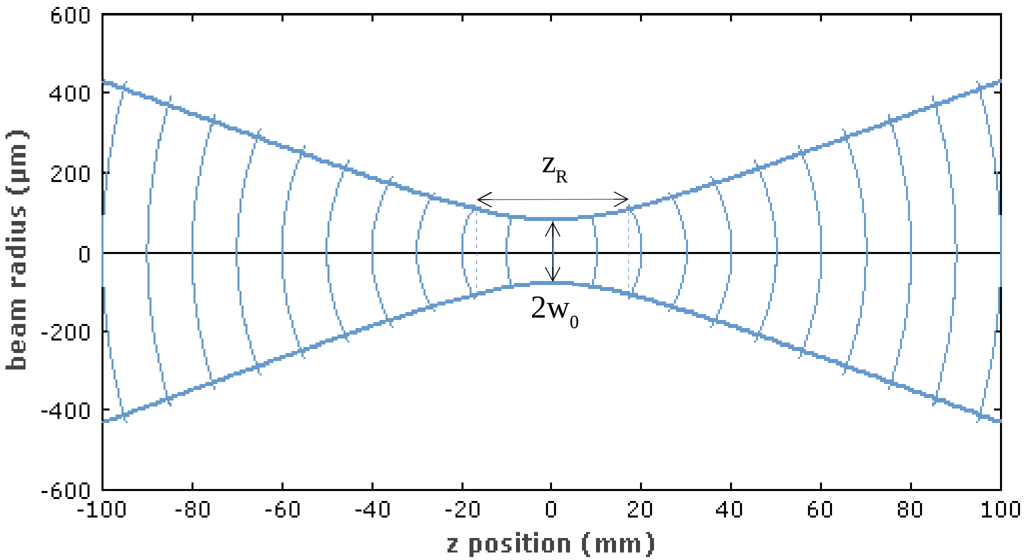

Figure 5: Gaussian beam with curved wavefront

Waist size: $w(z) = w_0\sqrt{1+\left(\frac{z}{z_R}\right)^2}$

Rayleigh length: $z_R = \frac{\pi w_0^2}{\lambda}$

Diverging angle: $\theta = \frac{\lambda}{\pi w_0}$

- A Gaussian beam has a minimum waist size w(z) depending on the beam wavelength, beam size and its position.
- It is basically governed by these three equations.
- Depending on the situation we want, we can manipulate the waist size using optical components.
- In this case, we want the minimum waist size to be located at the first mirror of the cavity.

3.1 Research on production cavity – Setup

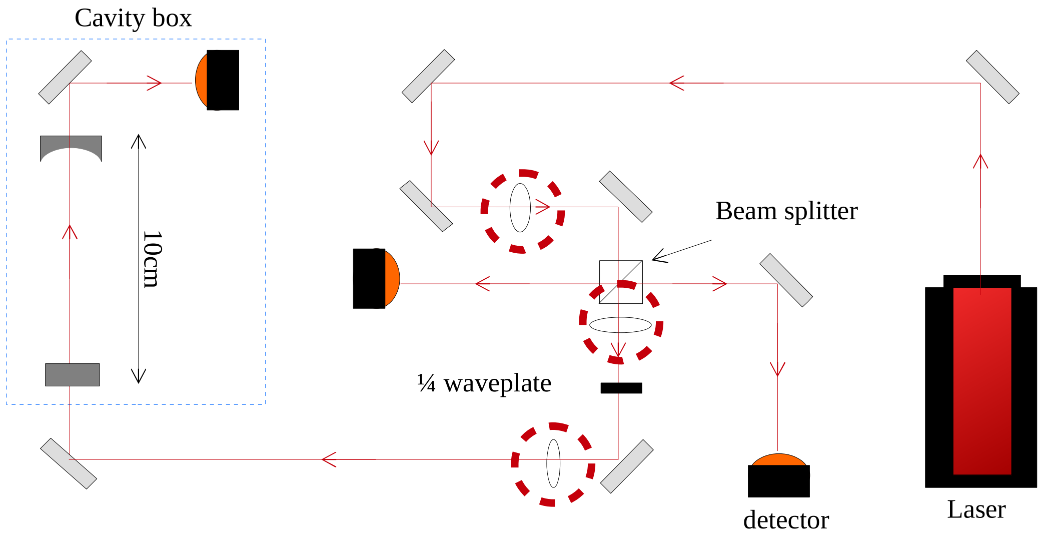

Figure 6: Optical set up for production cavity

- A Class 4 laser was used with wavelength of 1064nm.
- By simulation, the focal lengths and the positions of the lenses can be determined to locate the waist point at the first mirror of the cavity.
- A beam splitter and a ¼ waveplate were used to avoid back reflection by the cavity mirrors from damaging the laser.
- The two mirrors in the cavity are partially transparent in order to align the beam properly and to check whether the beam is still Gaussian.

3.1 Research on production cavity - Results

Figure 7: Gaussian mode beam produced by the cavity.

- Since the laser beam is a superposition of different modes, not only Gaussian mode will be produced.
- The cavity acts like a filter, depending on the length of the cavity, higher-order modes may be produced.

- After adjusting the length of the cavity and aligning the beam, a Gaussian mode was produced. Next step would be to fix the cavity with an offset and we will be in the position of testing our hypothesis

3.1 Research on production cavity - Results

Figure 7: Gaussian mode beam produced by the cavity.

- Since the laser beam is a superposition of different modes, not only Gaussian mode will be produced.
- The cavity acts like a filter, depending on the length of the cavity, higher-order modes may be produced.

- After adjusting the length of the cavity and aligning the beam, a Gaussian mode was produced. Next step would be to fix the cavity with an offset and we will be in the position of testing our hypothesis
- But we don't have an offset at the moment!

3.2 Coupling photons into an optical fibre

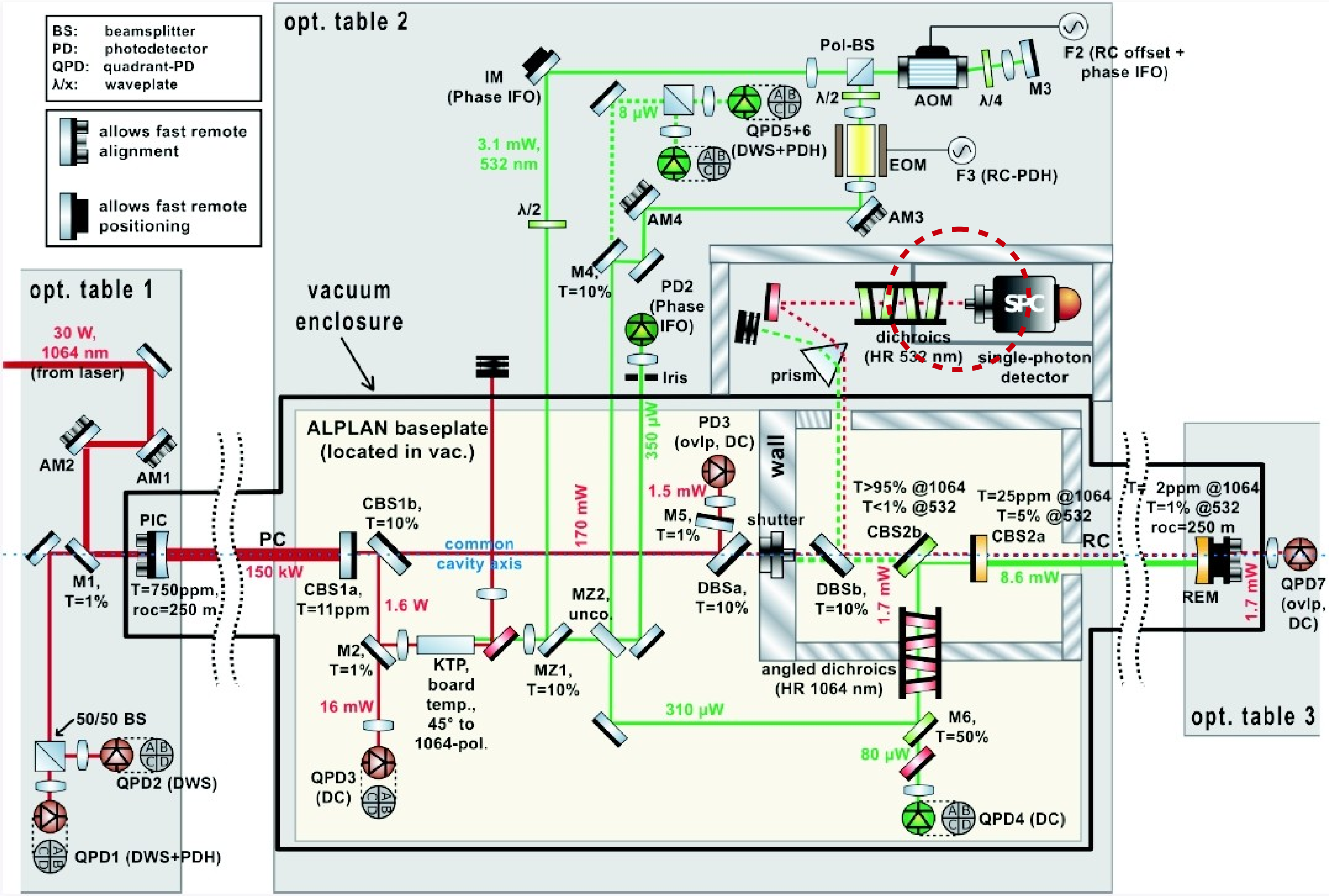

3.2 Coupling photons into an optical fibre

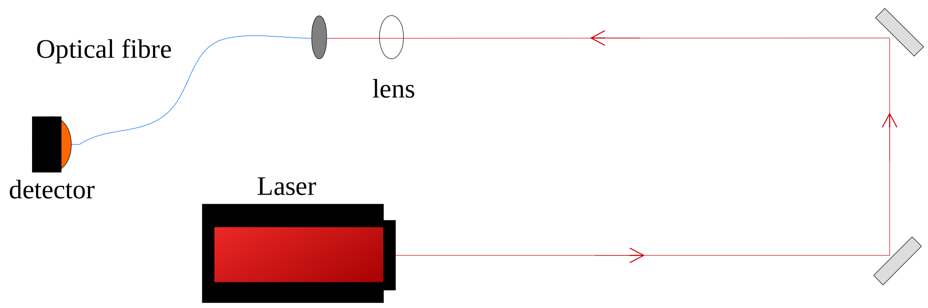

Figure 8: Optics setup for coupling photons into the optical fibre

- A connection that links the optics with the detector using optical fibre.
- Desirable to achieve over 80% efficiency. And it has achieved up to 53%.
- The task is to improve the coupling efficiency and to test the causes of loss in intensity.

- A He-Ne laser with a wavelength of 534nm was used. Two mirrors were used to introduce 4 degrees of freedom for adjusting the beam.
- Similar to the task before, a simulation was done to position the lens, due to the limiting lens, only the one with 25.4mm focal length could be used to focus the light into the optical fibre (so there will be some loss here).
- By using the walking-the-beam method, the coupling efficiency has improved up to 62%.
- It was observed that the fibre was glowing in the dark and there were reflections form the aperture of the fibre. These may explain the loss in the intensity especially when using laser beam with 1064nm.

3.3 A game designed and built for DESY open day

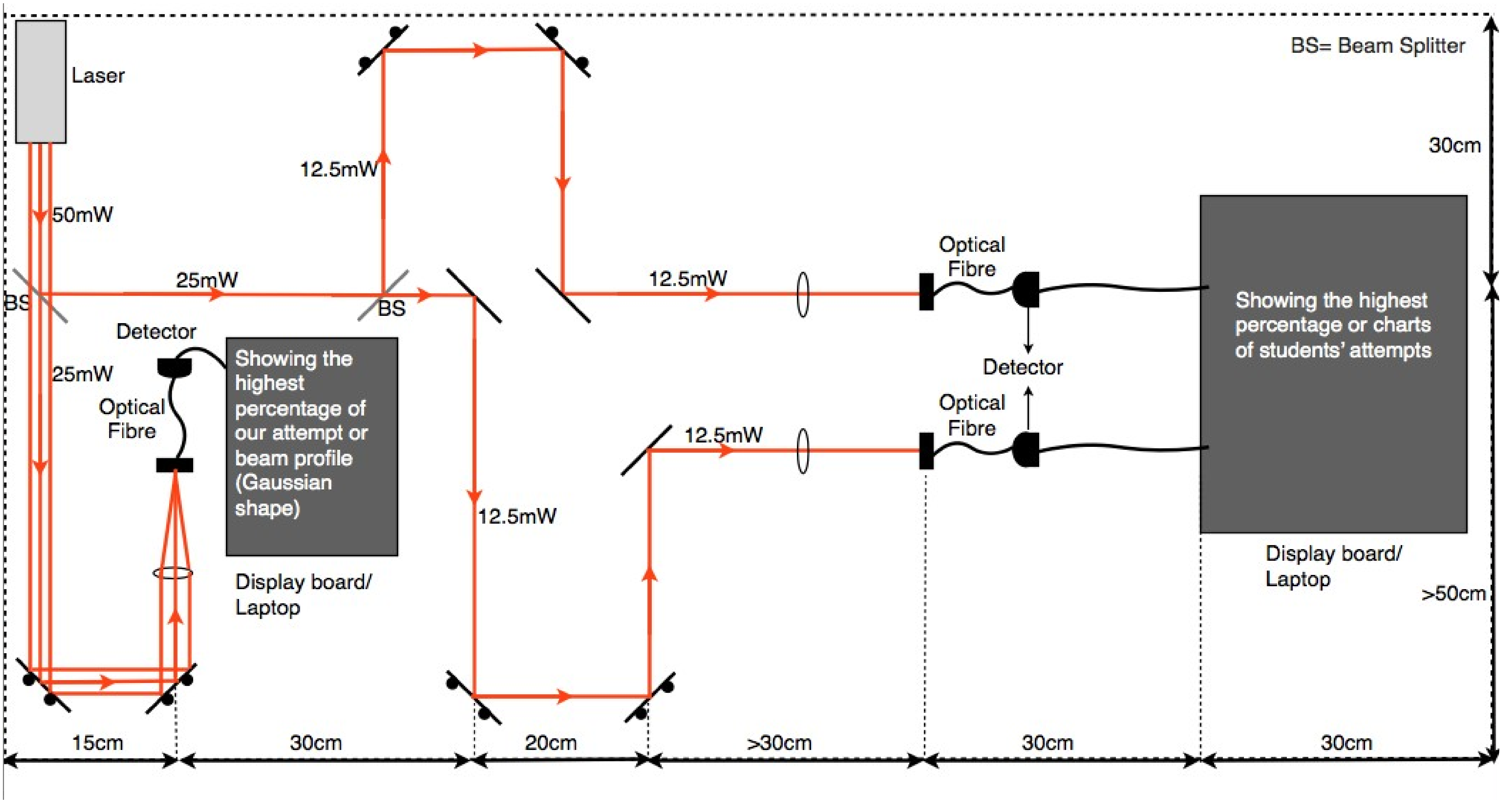

3.3 A game designed and built for DESY open day

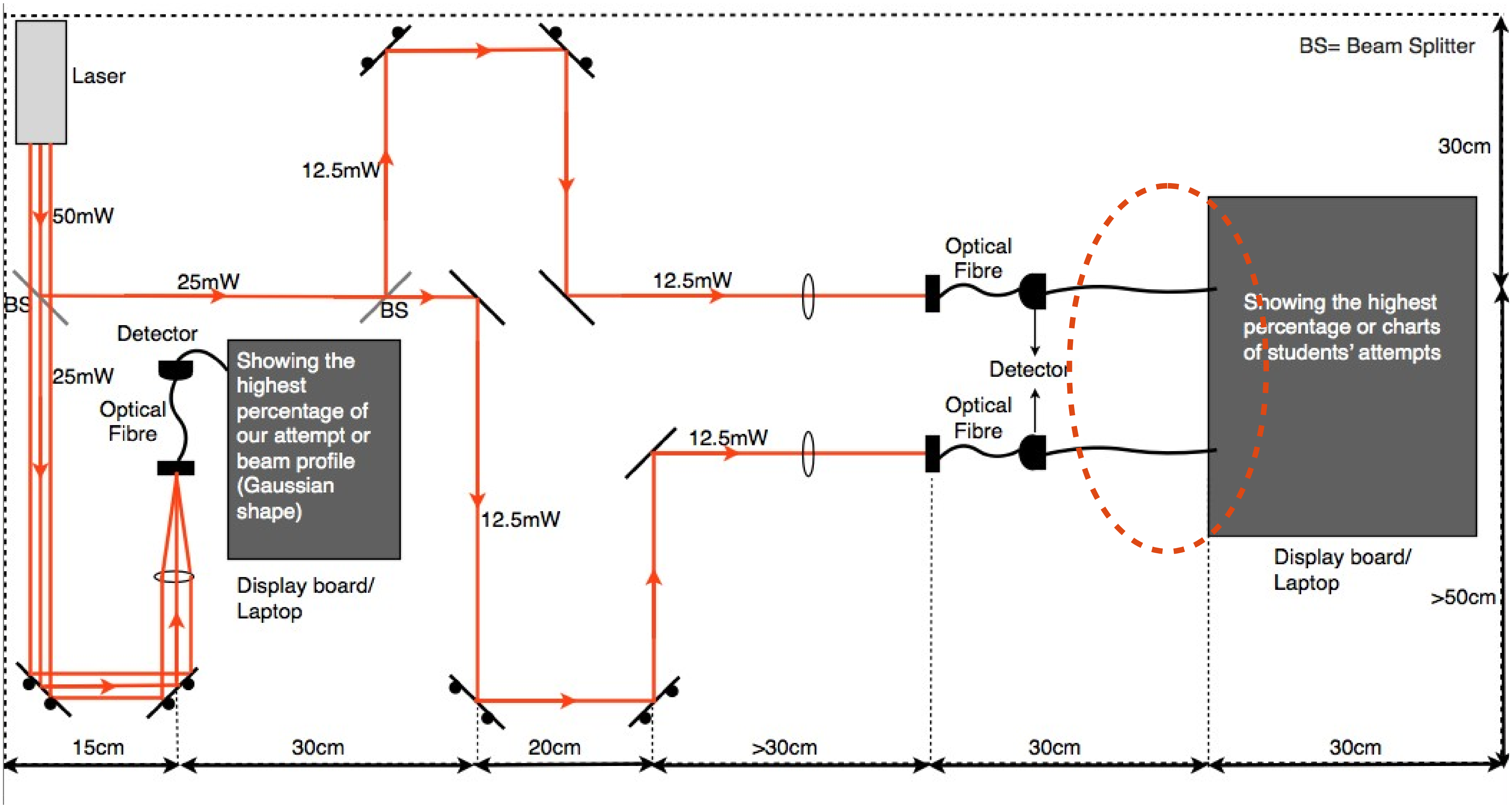

3.3 A game designed and built for DESY open day

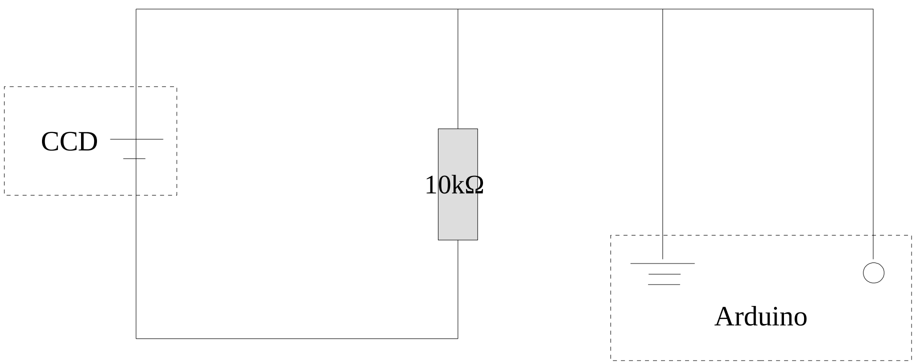

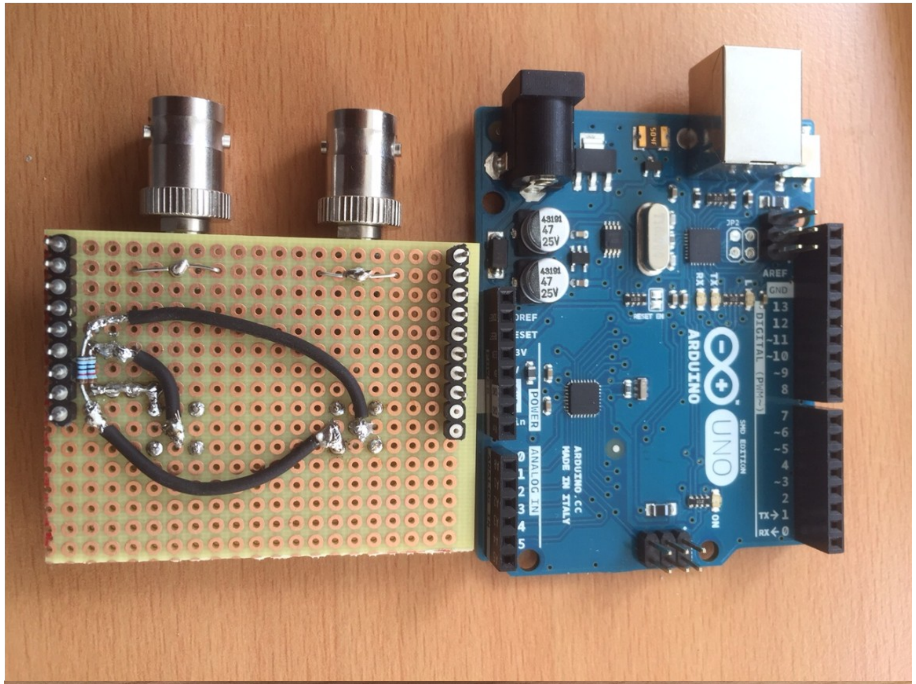

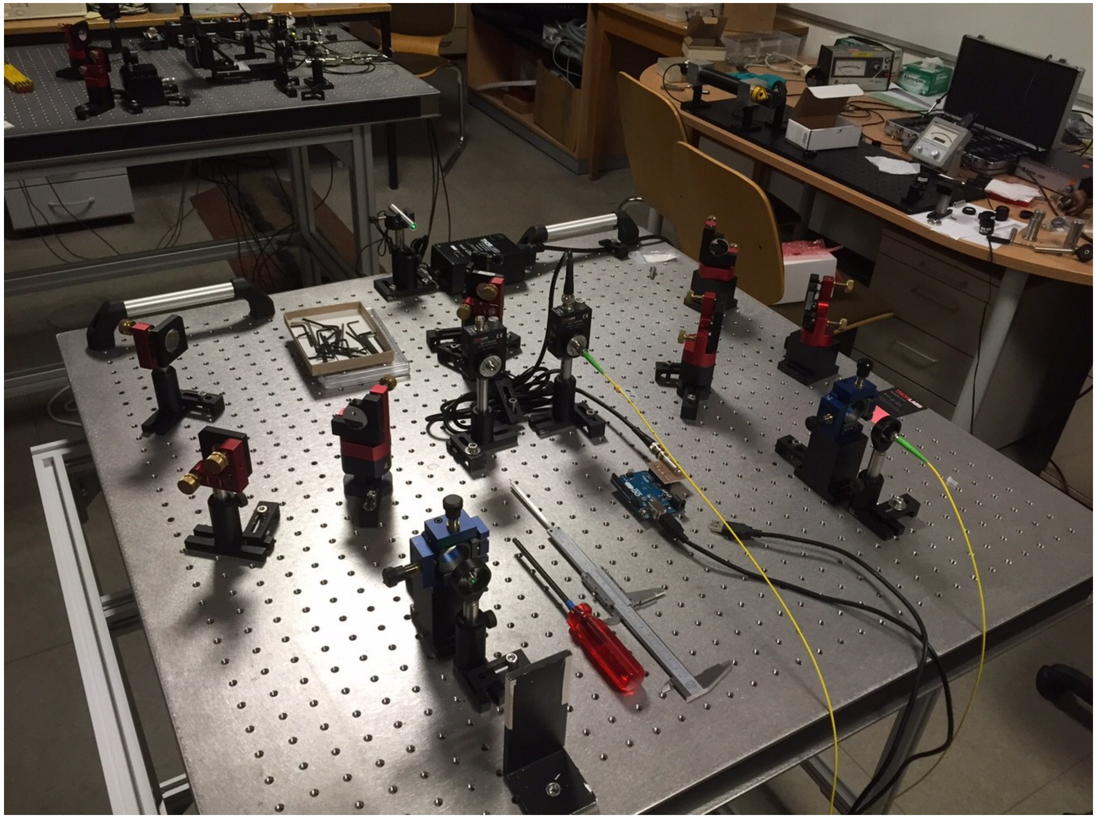

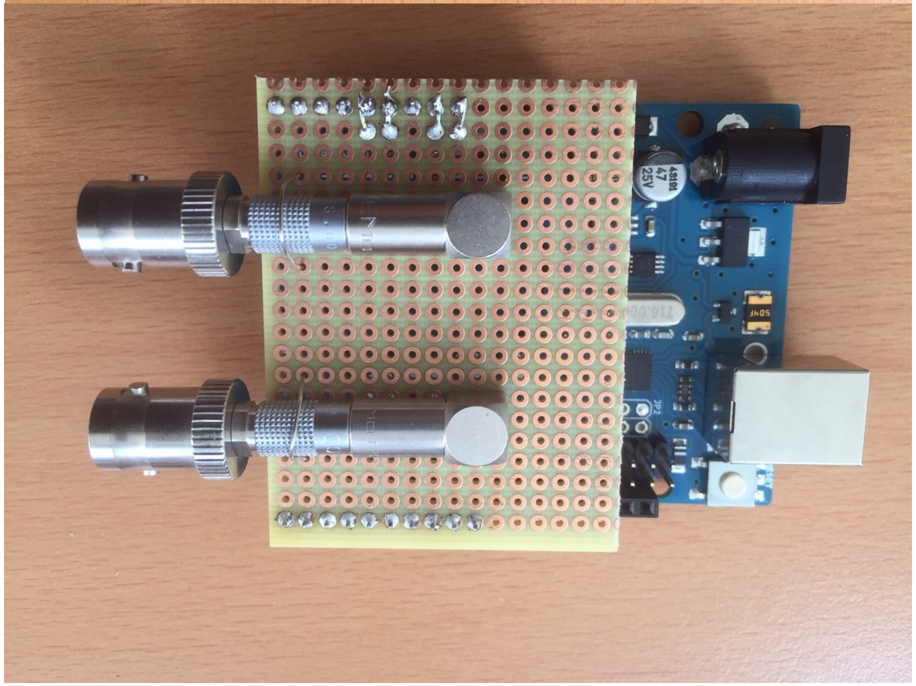

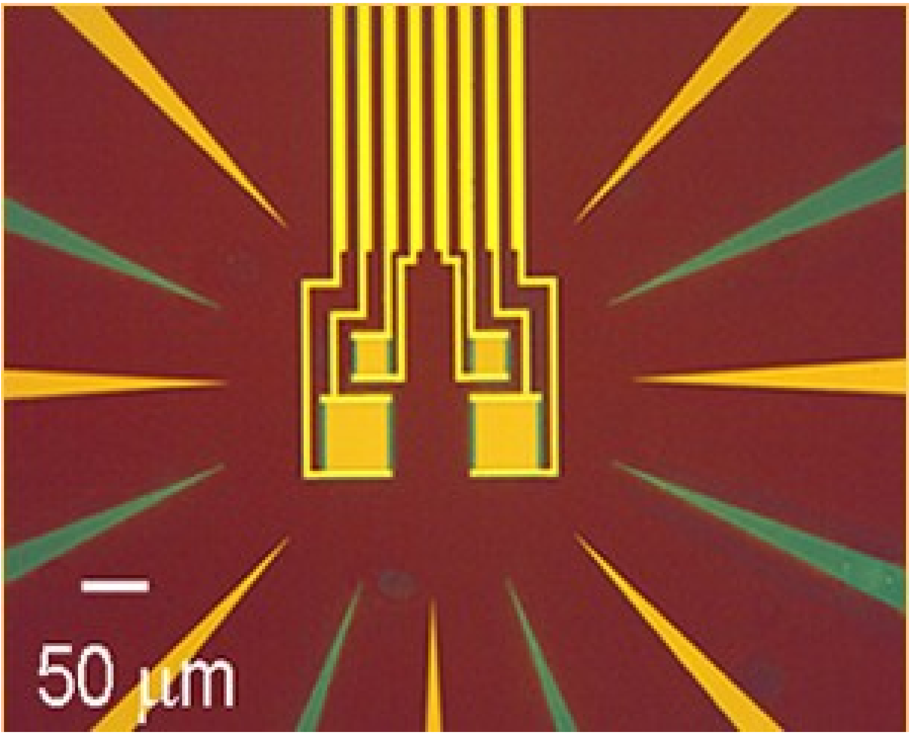

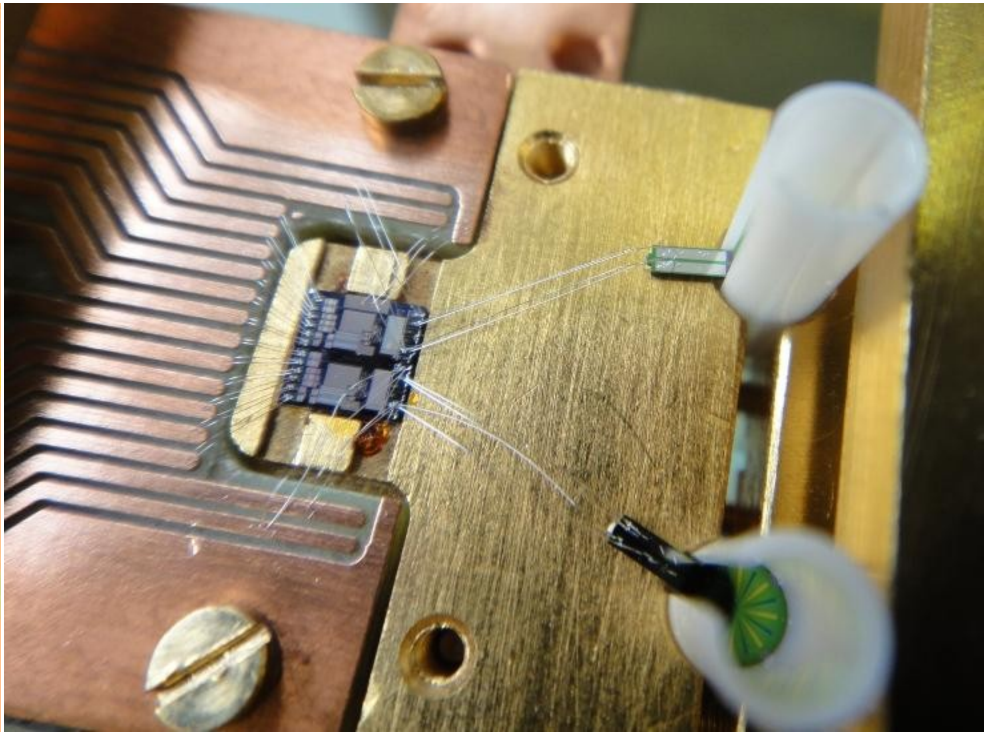

Figure 9: TES (left), TES with readout system SQUID (right)

The transition edge sensor (TES) is a type of cryogenic particle detector. It operates at very low temperature by using the principle of superconducting phase transition where a small raise in the temperature would result in a dramatic increase in its resistance.

The superconducting quantum interference device (SQUID) is a readout system in order to amplify the signal obtained from the TES.

4.1 Investigation of the black body photons sources

Problem:

- An unexpected signal with 1550nm was observed in the previous run (we are expecting only 1064nm)

Hypothesis:

- It might be due to the black body radiation coming from the heating bodies. So investigation on the sources of black bodies is needed.

Tests:

- Simulate the black body photons caused by different temperature and wavelengths using Python.
- Estimate the black body photons emitted by different heating bodies using IR camera.
- Build the shielding for protection

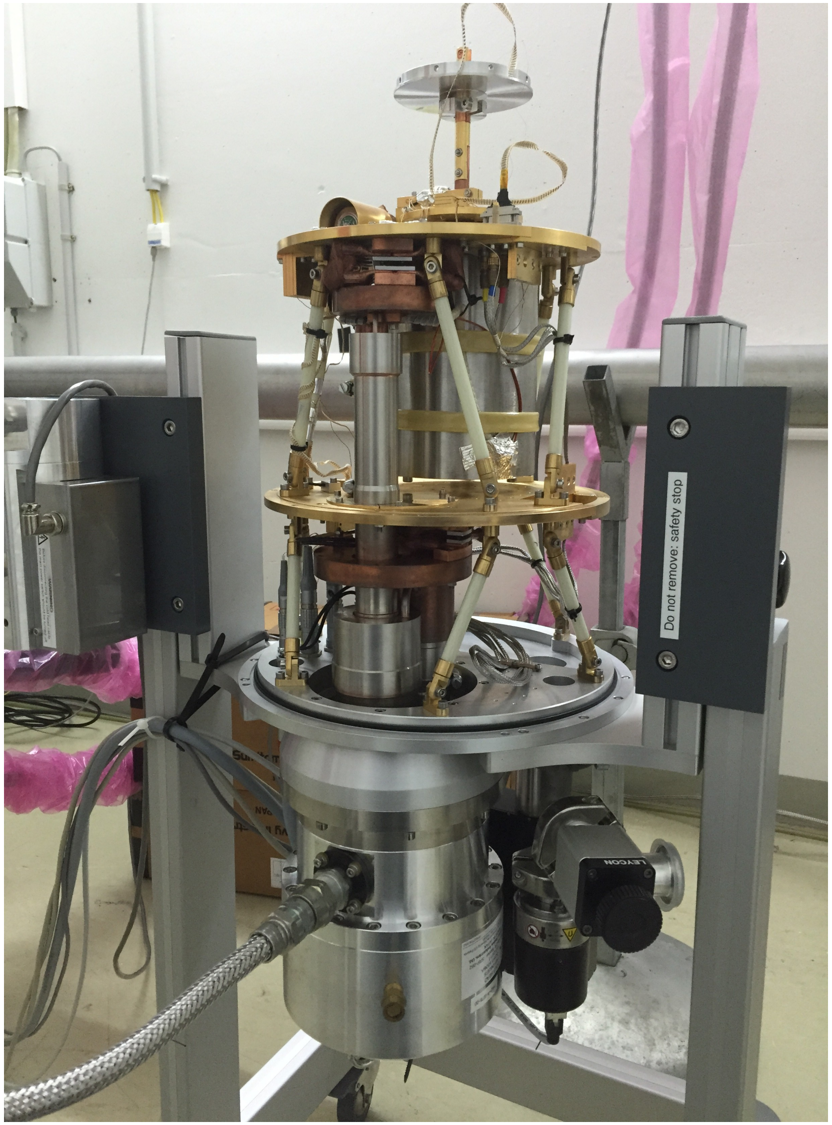

Figure 10: Cryostat with TES built in.

4.1 Investigation of the black body photons sources

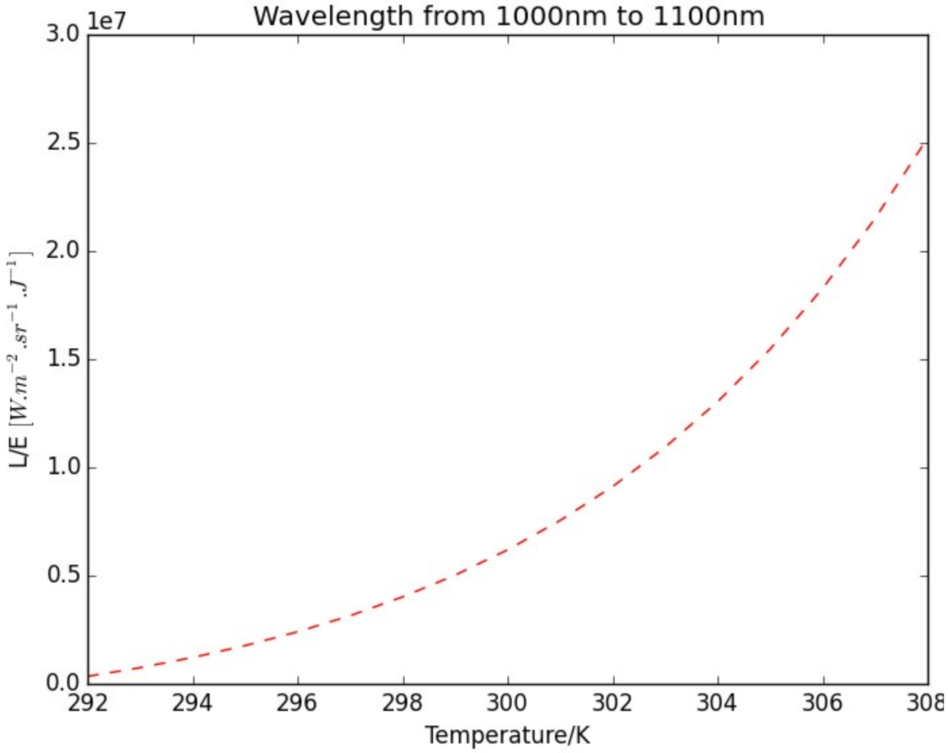

Figure 11: Rate of black body photons against temperature for wavelength between 1000 and 1100nm

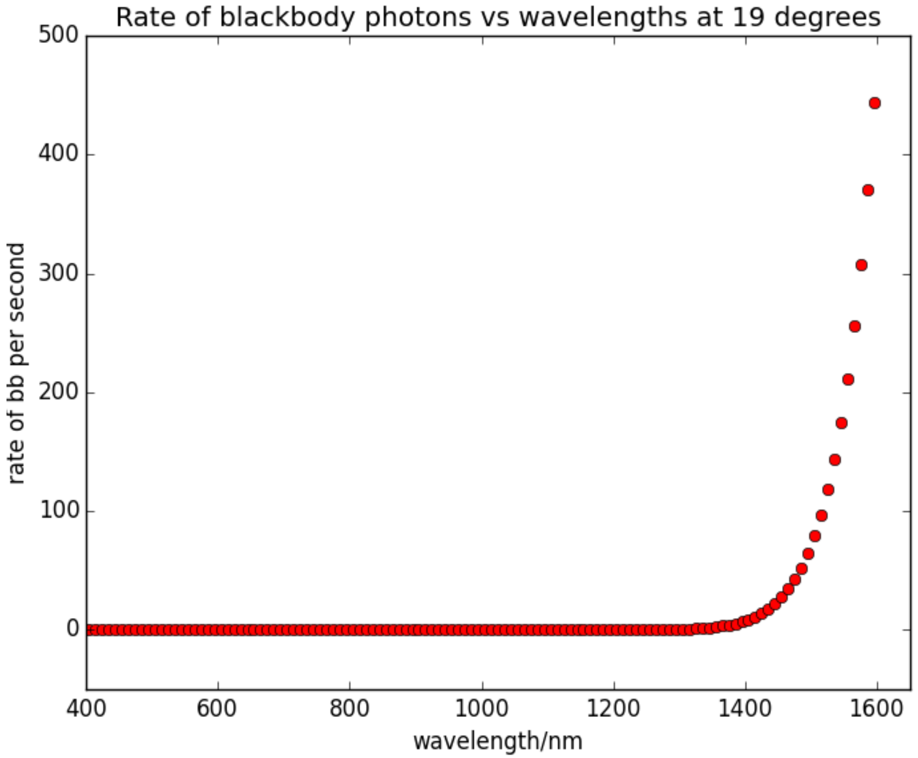

Figure 12: The rate of black body photons against wavelengths at lab temperature 19°C.

- The Gauss-Legendre method for evaluating the integration was used to simulate the black body photons. The rate of black body photons increases very quickly as the temperature increases.

- The rate of black body photons increases almost exponentially according to the wavelength. Thus, the photons with higher wavelength could be the dominating background.

4.1 Investigation of the black body photons sources

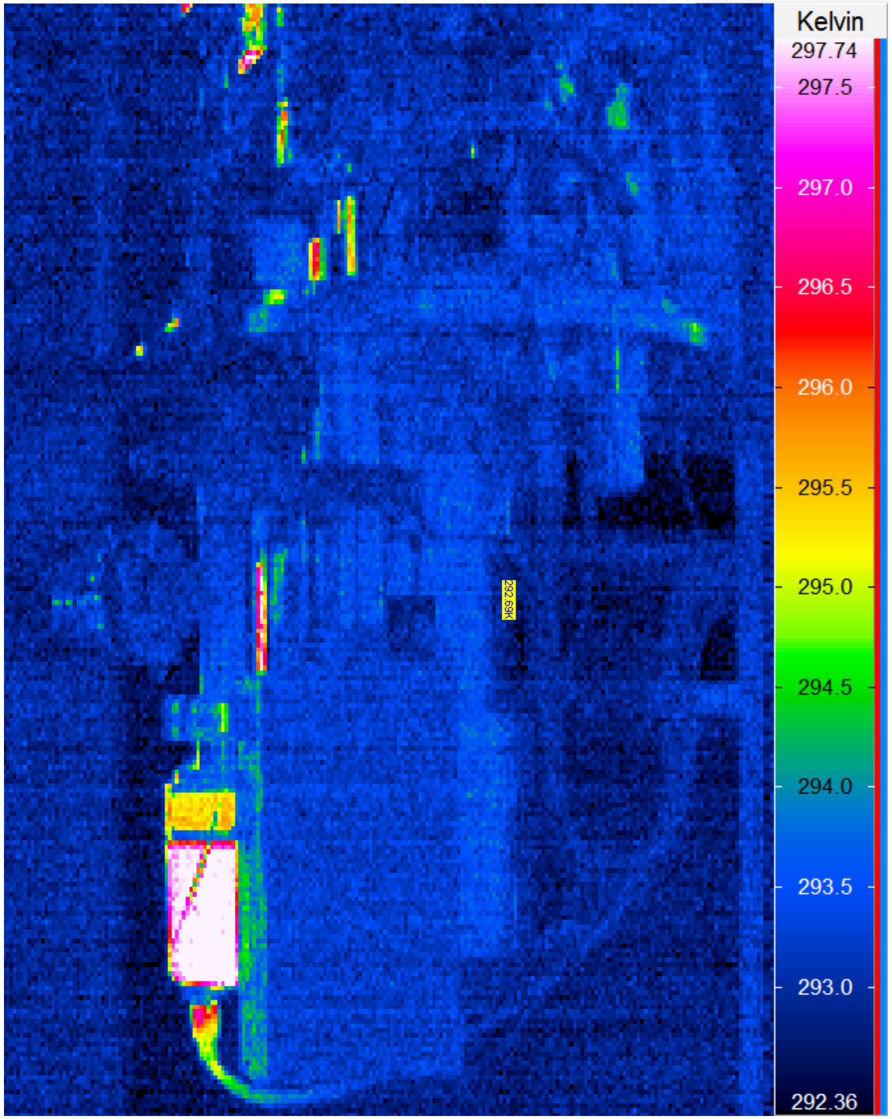

Figure 13: The picture of detector taken by IR camera with temperature scale.

4.1 Investigation of the black body photons sources

	Environment	Pressure sensor	Computer Screen	Control system	Oscilloscope	Light
Temperature /K	293.0	297.7	301.8	303.7	306.6	311.2
L/E ($W\ m^{-2} sr^{-1} J^{-1}$) for 1064nm	0.78×10^{6}	1.59×10^{6}	2.90×10^{6}	3.81×10^{6}	5.68×10^{6}	10.79×10^{6}
Rate of bbp (s^{-1})	1.57×10^{-3}	3.21×10^{-3}	5.85×10^{-3}	7.69×10^{-3}	11.50×10^{-3}	21.80×10^{-3}
L/E ($W\ m^{-2} sr^{-1} J^{-1}$) for 1550nm	0.35×10^{12}	0.58×10^{12}	0.88×10^{12}	1.06×10^{12}	1.40×10^{12}	2.18×10^{12}
Rate of bbp (s^{-1})	712.9	1169.9	1771.6	2140.2	2821.3	4397.2

NB: The L/E is the spectral radiance per photon energy, it is irrespective to the shape of the heating body.

4.2 Other tests for the detector

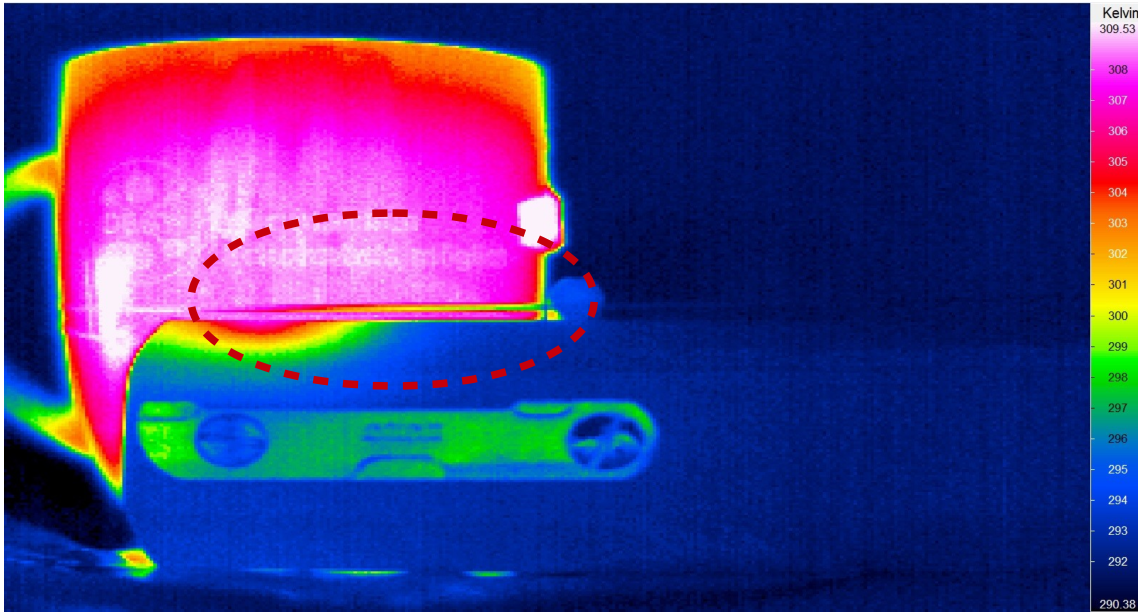

Figure 14: Temperature gradient of the fibre with a hot body and a cold body.

- The light-tightness shielding was repaired and tested for protecting the detector from other light sources.
- The temperature gradient of the fibre was measured to estimate how far and how long would it take for the optical fibre to have the same temperature as the environment between the 70K and the 4K stages of the ADR.
- A mechanical test was done to examine the protection for the optical fibre in order to maintain its efficiency.

5. Summary

- Searching for WISPs could prove the existence of dark matter.
- Theoretical prediction for the ALPS-II was produced by the theory group and they are building more theories beyond the standard model.
- The cavity needs to be further studied and the central part of the optics needs to be built in the next year.
- The unexpected signal from the last run could be explained by the black body photons. After eliminate all the possible sources, we will have a look again at the results from next run.
- There are still many obstacles to be overcome in the next few years in both optics and detector.
- After solving most of the problems, the magnets from HERA tunnel will be reused to cover the cavities for detecting axion. Then we are at the stage of detecting WISPs!

Thank you!